Correlations between the Structure and Dielectric Properties of $Pb(Sc_{2/3}W_{1/3})O_3$ – $Pb(Ti/Zr)O_3$ Relaxors

Pavol Juhás*, Wojtek Dmowski*, Ilya Grinberg†, Takeshi Egami*, Andrew M. Rappe† and Peter K. Davies*

*Dept. of Materials Science and Engineering, University of Pennsylvania, Philadelphia, PA 19104
†Dept. of Chemistry, University of Pennsylvania, Philadelphia, PA 19104

Abstract. The effects of Ti and Zr on the structure and ordering in the $(1-x)Pb(Sc_{2/3}W_{1/3})O_3$ – $(x)PbTiO_3$ (PSW–PT) and $(1-x)Pb(Sc_{2/3}W_{1/3})O_3$ – $(x)PbZrO_3$ (PSW–PZ) systems were studied using synchrotron x-ray and neutron diffraction. Rietveld refinement was carried out to determine the average long-range crystallographic structure and pair distribution function (PDF) analysis to probe the local displacements of the atoms. For $x < 0.25$ the B-cations form a 1:1 ordered doubled perovskite structure (space group $Fm\bar{3}m$). The refined occupancies were consistent with the "random site model", where the ordered structure consists of one B-sublattice occupied by Sc and the other by a random mixture of the remaining cations. The B-site order is reduced by incorporation of Zr, but highly stabilized by Ti with the degree of order in excess of 95% for $x \leq 0.25$. The results of PDF analysis show that on the local scale the Pb and O atoms are significantly displaced from their average lattice positions. The PDF curves were simulated by several models of simple Pb and O shifts. The short-range PDF of PSW could be approximated by allowing Pb shifts along [100] and rotations of BO_6 octahedra around $[10\bar{1}]$. This model was inadequate for a longer distances ($r > 4.25$ Å) suggesting the real cation displacements are more complicated. Distortions of the local structure in the PSW–PT system were modeled also by density functional theory calculations. The obtained magnitudes of local Pb displacements coincide with the temperature of paraelectric transition $T_{\varepsilon,max}$.

1. INTRODUCTION

The dielectric and piezoelectric properties of the lead based $PbBO_3$ perovskites show great variance with the composition and structural order of the B-site cations. Although the B-site chemistry is critical for the overall dielectric response of these systems, signifi cant contributions come from the shifts of the A-site Pb cations. The magnitude and direction of these displacements is determined by the Pb environment, in particular by the oxygen neighbors. The Pb–O bonds are influenced by bonding of oxygen to its nearest B-site neighbors, and as a result oxygens mediate the interaction between Pb displacements and B-site chemistry. The exact relationship between structure and dielectric response is complicated and driven by many coupled interactions. We have attempted to investigate these relations in the two solid solutions of $Pb(Sc_{2/3}W_{1/3})O_3$–$PbTiO_3$ (PSW–PT) and $Pb(Sc_{2/3}W_{1/3})O_3$–$PbZrO_3$ (PSW–PZ). These systems appeared to be convenient for such study, because in spite of similar chemistries they show a completely different response to the B-site substitution.

CP677, *Fundamental Physics of Ferroelectrics 2003*, edited by P. K. Davies and D. J. Singh
© 2003 American Institute of Physics 0-7354-0146-2/03/$20.00

Downloaded 02 May 2005 to 165.123.34.86. Redistribution subject to AIP license or copyright, see http://proceedings.aip.org/proceedings/cpcr.jsp

PSW is similar in properties to the $Pb(Mg_{1/3}Nb_{2/3})O_3$ (PMN) family of compounds, since it displays a relaxor type response and forms a B-site ordered structure with 1:1 rock salt periodicity. The effects of cation substitutions and thermal treatments on the B-site order and dielectric properties in $(1-x)Pb(Sc_{2/3}W_{1/3})O_3-$ $(x)PbTiO_3$ and $(1-x)Pb(Sc_{2/3}W_{1/3})O_3-$ $(x)PbZrO_3$ have been previously reported [1]. The results indicated that the 1:1 $Pb[\beta'_{1/2}\beta''_{1/2}]O_3$ order in PSW can be represented by a modifi ed "random site" structure. According to this model, the structure of the fully ordered PSW end-member can be represented as $Pb[Sc]_{1/2}[Sc_{1/3}W_{2/3}]_{1/2}O_3$ and the ordered solid solutions by $Pb[Sc]_{1/2}[Sc_{(1-4x)/3}W_{(2-2x)/3}M_{2x}]_{1/2}O_3$, where M^{4+} is either Zr or Ti. Because of the $(1-4x)/3$ term, this substitution pattern for the solid solutions is only possible for $x \leq 0.25$, for $x > 0.25$ the M^{4+} cation must substitute on both lattice sites, to give stoichiometries with $Pb[Sc_{(4-4x)/3}M_{(4x-1)/3}]_{1/2}[W_{(2-2x)/3}M_{(2x+1)/3}]_{1/2}O_3$. The order parameter of PSW–PT and PSW–PZ samples has been evaluated from the conventional powder x-ray diffraction (XRD) by comparing the measured intensity of the (111) reflection to its calculated value, see Fig. 1. For PSW–PT the cation order was found to be much more stable and to extend to higher substitution levels compared to its PSW–PZ counterpart. This observation could be interpreted in terms of the radii difference of the ordered sites predicted by the random site model - which increase with x for the Ti system, but decrease for the substitution of Zr. All of the investigated compositions showed relaxor ferroelectric behavior, however PSW–PT displayed unusual trends in the temperature of the permittivity maximum $T_{\varepsilon,max}$, which decreased for $x \leq 0.2$ and then increased for $x > 0.25$. In contrast, for the PZ system $T_{\varepsilon,max}$ varies linearly with the Zr content, as displayed in Fig. 2. These observations can be rationalized in terms of the B-site occupancies predicted by the random site model. For the substitution of PT complete order occurs for $x \leq 0.25$ (Fig. 1), therefore one lattice site (β') is occupied exclusively by Sc and the other (β'') by a mixture of Sc, W and Ti. However for $x > 0.25$ Ti must substitute on both ordered sites and the presence of Ti–O–Ti or Ti–O–W bonds becomes likely. It is precisely at this composition where the sharp growth in $T_{\varepsilon,max}$ is observed - Fig. 2. The appearance of Ti–O–Ti and Ti–O–W neighbors can induce longer range coupling of the ferroelectrically active Ti^{4+} and W^{6+} cations. It is also possible that over-bonding of oxygens in Ti–O–W and Ti–O–Ti may alter the directions and magnitudes of lead displacements. For PSW–PZ the degree of order is less than 100% even for low substitution rates, implying that both ordered sites contain a mixture of several cations. Consequently there is no abrupt change in the pattern of B-site occupation and the linear behavior of $T_{\varepsilon,max}$ versus x is not unexpected.

Our previous data strongly supported the random site model as a correct description of the ordered PSW–PT and PSW–PZ compounds. Nevertheless more detailed structure analysis was necessary to reliably determine the B-site occupancies and to probe the alterations in the atomic displacements that accompany the changes in composition, order and dielectric response. Therefore we performed a detailed Rietveld and pair distribution function (PDF) studies of the PSW–PZ and PSW–PT systems using synchrotron x-ray and neutron diffraction (ND).

Downloaded 02 May 2005 to 165.123.34.86. Redistribution subject to AIP license or copyright, see http://proceedings.aip.org/proceedings/cpcr.jsp

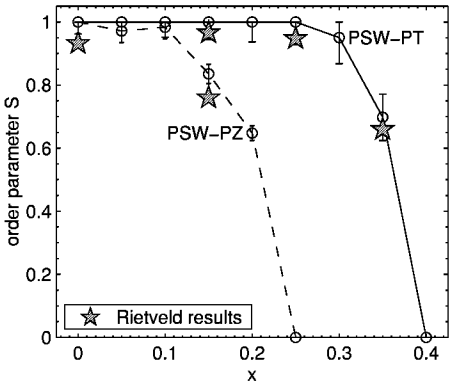

FIGURE 1. Degree of order S vs. composition x for PSW–PZ and PSW–PT.

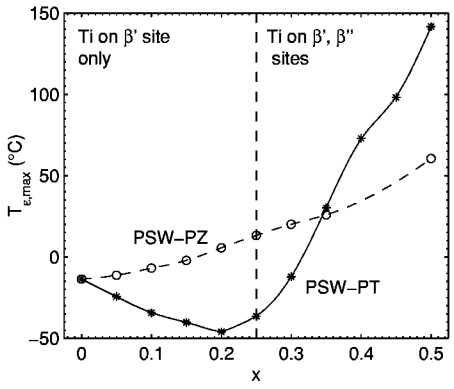

FIGURE 2. Variation of $T_{\varepsilon,max}$ (1MHz) with x for PSW–PT and PSW–PZ.

2. EXPERIMENTAL PROCEDURES

Samples of $(1-x)$PSW – (x)PT, $x = 0$, 0.15, 0.25, 0.35 and $(1-x)$PSW – (x)PZ, x = 0.15, 0.35 were prepared by solid-state methods from high-purity oxides (> 99.9%) via the "columbite route". The annealing treatment was conducted in a way known to maximize the B-site order. The details of the sample preparation are reported elsewhere [1]. X-ray diffraction data were measured using the beamline X7A at the National Synchrotron Light Source (NSLS), Brookhaven National Laboratory. Powder samples were placed in a 0.1 mm glass capillaries, which were rotated during the measurement to improve orientational averaging. A constant wavelength of $\lambda = 0.50095$ Å was selected using a Ge (111) monochromator. Diffraction intensities were measured by a position sensitive detector in the Q range of 1.1 $Å^{-1}$ - 10 $Å^{-1}$ ($d = 0.62$ Å - 5.8 Å). The data were analyzed by Rietveld method using the GSAS software package [2]. The Bragg reflections were fi tted by an asymmetric peak profi le function #3. The wider profiles of ordering reflections were modeled using the GSAS procedure for stacking fault broadening, which introduced additional broadening terms for the reflections outside of {200} sub-lattice. The scale factor, background function, lattice constant, profile coeffi cients, temperature factors, oxygen position and B-cation occupancies were all refi ned together.

Neutron diffraction time of flight experiments were performed at the SEPD beamline at the Intense Pulse Neutron Source (IPNS), Argonne National Laboratory. The diffraction data were measured for 5 hours at 20 K and 290 K. The incident spectrum and scattering effects from the specimen chamber were calibrated by runs using vanadium rod and empty sample container. The diffraction data were analyzed by Rietveld and pair distribution function methods. The Rietveld analysis was carried out using data from the 144.85° detector bank in the Q range of 1.88 $Å^{-1}$ - 15.7 $Å^{-1}$ (d range 0.4 Å - 3.35 Å). The additional broadening of the ordering reflections was facilitated by the GSAS stacking fault model for the {200} sub-lattice. The lattice parameter, background function, profi le coeffi cients, B-site occupancies, temperature factors and oxygen po-

Downloaded 02 May 2005 to 165.123.34.86. Redistribution subject to AIP license or copyright, see http://proceedings.aip.org/proceedings/cpcr.jsp

TABLE 1. Results of Rietveld analysis of XRD ([x]) and ND ([n]) patterns from PSW–PT and PSW–PZ.

x	a (Å)	S	Δz_O (a)	U_{Pb}	$U_{O\perp}$	$U_{O\parallel}$	U_B (Å^2)	R_{F^2} (%)	R_{wp} (%)
0 [x]	8.1349	0.933	0.0054	0.055	0.034	–	0.0039	6.7	4.0
0 [n]	8.1360	0.847	0.0082	0.049	0.029	0.006	0.0054	40	4.5
0.15Ti [x]	8.1011	0.969	0.0075	0.043	0.017	–	0.0033	9.7	3.7
0.15Ti [n]	8.0994	0.802	0.0080	0.048	0.023	0.005	0.0056	36	4.4
0.25Ti [x]	8.0761	0.948	0.0073	0.048	0.023	–	0.0081	6.8	4.0
0.25Ti [n]	8.0785	0.644	0.0073	0.047	0.020	0.006	0.0056	36	4.3
0.35Ti [x]	8.0593	0.659	0.0069	0.050	0.039	–	0.0110	8.0	3.6
0.35Ti [n]	8.0619	0.516	0.0038	0.047	0.022	0.009	0.0043	42	4.4
0.15Zr [x]	8.1615	0.760	0.0041	0.059	0.044	–	0.0120	7.1	3.4
0.15Zr [n]	8.1644	0.589	0.0055	0.049	0.035	0.008	0.0055	42	4.7
0.35Zr [x]	8.1953	0	–	0.051	0.045	–	0.0090	6.9	2.5
0.35Zr [n]	8.2050	0	–	0.053	0.043	0.009	0.0056	37	5.4

sitions were all refi ned together. For the PDF analysis, the scattering intensities were re-grouped to 5 detector banks at 21.8°, 44.0°, 90.0°, 139,7° and 150.0°, which allowed good intensity in the Q range of 1.2 Å^{-1} - 30 Å^{-1}. The experimental PDF curves were calculated from raw intensities using the PDFGetN software, and the PDF simulations were carried out using the PDFFit program [3, 4].

3. RESULTS

3.1. Rietveld Refinements

Results of the Rietveld refi nement for the XRD and ND spectra of PSW are displayed in Fig. 3. The ordering reflections were observed in all samples (PSW–PT, $x = 0.0$, 0.15, 0.25, 0.35 and PSW–PZ $x = 0.15$) with the exception of PSW–PZ, $x = 0.35$. There was no sign of peak splitting in any of the measured x-ray or neutron spectra at 20 K or 290 K and all diffraction patterns were consistent with the cubic perovskite structure. The samples displaying B-site order were refi ned using the doubled perovskite structure, space group $Fm\bar{3}m$. A simple perovskite lattice, ($Pm\bar{3}m$) was used for disordered (0.65)PSW–(0.35)PZ. The total occupancies of all lattice sites were fi xed to 1, and the occupancies of the B-cations were required to satisfy the overall stoichiometry. Such conditions permit 2 free parameters for the B-chemistry. However, only one can be refi ned, since all structure factors of ordering reflections are proportional to the same value ($F_{ord} \approx f_{\beta'} - f_{\beta''}$). Therefore the B-occupancies were set to linearly change with a single parameter S from a completely random structure ($S = 0$) to the one with maximum order at $S = 1$. The oxygen positions were refi ned in accordance to the $Fm\bar{3}m$ symmetry, which allows O shifts along β'–O–β'' bonds. XRD data were simulated using isotropic temperature coeffi cients with a common value for all B-cations. In the case of neutron diffraction, which can access wider Q range, separate temperature coeffi cients were used for the β' and β'' sites, and the O factors were refi ned as anisotropic with components perpendicular ($U_{O\perp}$) and parallel ($U_{O\parallel}$) to the β'–O–β'' bond. The refi ned lattice con-

Downloaded 02 May 2005 to 165.123.34.86. Redistribution subject to AIP license or copyright, see http://proceedings.aip.org/proceedings/cpcr.jsp

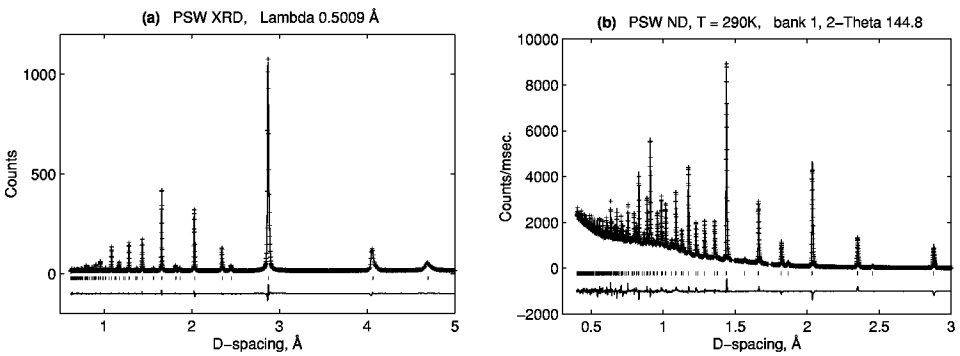

FIGURE 3. Rietveld refinement of **(a)** x-ray and **(b)** neutron diffraction patterns of PSW.

stants, order parameters S, the oxygen shifts Δz_O from β' to β'' and temperature factors U for XRD and ND spectra at 290 K are listed in Table 1.

All of the model structures could be refi ned to an excellent agreement with the experimental data, with the fi nal residua $R_{wp} \approx 4\%$. The values of order parameter S obtained from neutron refi nements were considerably smaller than their XRD counterparts. Because the fi nal residua of structure factors R_{F^2} for XRD were an order of magnitude smaller than for ND (Table 1), the order parameters S from the XRD data should be considered reliable, and they also agree very well with the previous results, Fig. 1. The Rietveld analysis confi rmed essentially complete order in PSW–PT for $x \leq 0.25$ and proved that the random site model is a correct description of the B-chemistry in PSW–PT and PSW–PZ systems. This model is also the arrangement that maximizes the x-ray intensities of the super-reflections, because Sc has the lowest atomic number of all B-cations ($F_{ord} \approx f_{\beta'} - f_{\beta''}$). Thus it is very unlikely that any other B-site structure could equally well simulate the observed strong intensities of the ordering reflections.

The large values of R_{F^2} for the ND refi nements probably arise from the many overlapping peaks for high Q. While the wide Q range appears unfavorable for the occupancies, it allows better accuracy for the temperature coeffi cients. The R_{wp} factors for the neutron data were considerably improved by using anisotropic temperature factors for O and attributing separate values of U to the ordered β-sites. The refi ned temperature factors of Pb and O were very high and they correspond to an unrealistically large magnitudes of vibrations of $\sim$0.22 Å for Pb and $\sim$0.17 Å for O. Contrary to the expectations, the temperature factor of Pb in (0.75)PSW–(0.25)PT decreased from $\sim$0.052 Å^2 to $\sim$0.047 Å^2 after heating from 20 K to 290 K. This indicates that large Debye-Waller factors were not due to temperature vibrations, but they were rather caused by a local displacements of Pb and O atoms from their average lattice positions. These shifts are not correlated over larger distances, therefore the long range structure remains cubic, however they show up as increased temperature factors. The increase in U_{Pb} at low temperatures can be explained by the Pb shifts becoming more correlated and less likely to flip. For the O atoms, the temperature factor $U_{O\|}$ along the B–O bond is 2 - 4 times smaller than the perpendicular component $U_{O\perp}$. This suggests that local O shifts occur mainly in the directions transversal to B–O, which could correspond to rotations of the BO_6 octahe-

Downloaded 02 May 2005 to 165.123.34.86. Redistribution subject to AIP license or copyright, see http://proceedings.aip.org/proceedings/cpcr.jsp

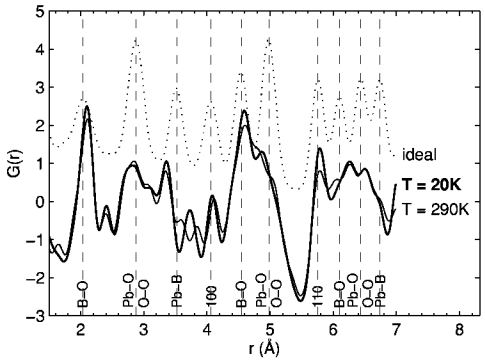

FIGURE 4. PDF curves for PSW at 20 K – thick line, and at 290 K – thin line. Dotted line denotes PDF calculated for the Rietveld - refined structure.

dra. The temperature coeffi cients for B-cations have reasonable values and they were found to increase with temperature. All of the refi ned Δz_O were positive and indicated off-centering of oxygen away from the β' site, which is rich in the larger Sc cations.

3.2. Pair Distribution Function Analysis

The Pair Distribution Function (PDF) provides information about inter-atomic distances in the material and it is obtained by Fourier transformation of the entire diffraction spectrum. The usage of PDF for a crystalline materials is discussed elsewhere [5, 6, 7]. In this paper the PDF is expressed through the function $G(r)$ defi ned as

$$G(r) = \frac{1}{Nr}\sum_{i,j}\left[\frac{b_i b_j}{\langle b\rangle^2}\,\delta(r-r_{ij})\right] - 4\pi r\rho_0$$

where b is the neutron scattering length and r_{ij} is a distance of i and j atoms. Fig. 4 shows the experimental PDF curves of PSW obtained by neutron scattering at 20 K and 290 K. The dotted line on top is the PDF calculated for the average Rietveld structure and the vertical grid marks the expected bond lengths. The experimental PDF curves are considerably different from the calculated one and confi rm a signifi cant distortion of the local structure from the average lattice. The fi rst peak of $G(r)$ at 2.1 Å is due to the B–O nearest neighbors, and has a full width at half maximum of ~0.21Å. This width is only slightly higher than the difference of the ionic radii of Sc^{3+} and W^{6+} ($\Delta R_\beta = 0.145$, $r_{Sc^{3+}} = 0.745$, $r_{W^{6+}} = 0.60$), which indicates that there is no signifi cant off-centering of the B-cations. This conclusion is supported by the Rietveld analysis, which yielded small temperature coeffi cients for the B-cations. Therefore it can be assumed that the B-cations are fi xed at their average positions. While the fi rst PDF peak showed fair agreement with the calculated curve, there were considerable differences for the second and third peaks. The second nearest distance of Pb–O and O–O pairs is split to at least 3 overlapping peaks at 2.4 Å, 2.8 Å and 3.1 Å. This splitting is unlikely due to the O–O bonds, because distortions of BO_6 octahedra would display also in the fi rst B–O peak. As a result there

Downloaded 02 May 2005 to 165.123.34.86. Redistribution subject to AIP license or copyright, see http://proceedings.aip.org/proceedings/cpcr.jsp

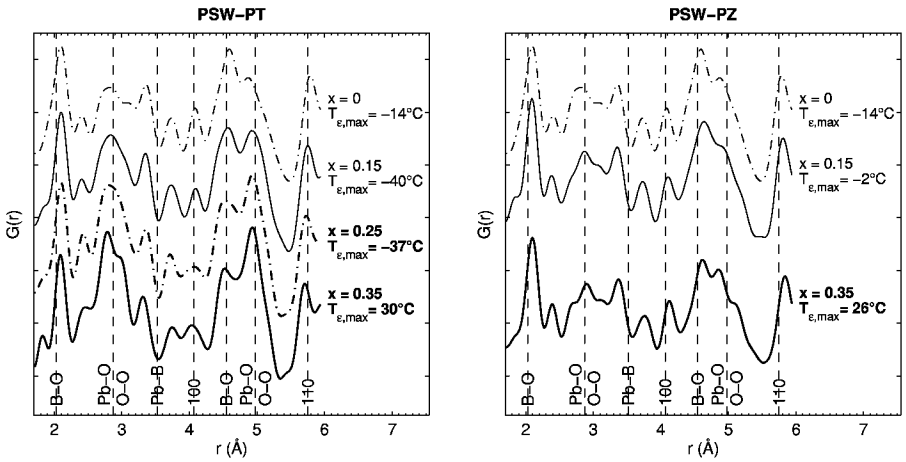

FIGURE 5. PDF curves for PSW–PT and PSW–PZ at 20 K. Composition and $T_{\varepsilon,max}$ values are noted on the right side of plots.

must be a large variance in the Pb–O bond lengths, which may arise from the shifts of Pb cations or from the rotations of the BO_6 octahedra. Lead displacements are confi rmed by the third nearest distance of Pb–B, which is divided between 2 peaks at ~3.4 Å and ~3.7 Å. The $G(r)$ curves measured at 20 K and 290 K were quite similar, however they had a noticeable difference at $r \approx 3.5$ Å, corresponding to the Pb–B neighbors. The two peaks of the Pb–B lengths at 20 K become more spread with the heating to 290 K, and eventually create 3 maxima in the PDF. Increased temperature thus seems to add more options and larger randomness to the Pb displacements.

Effect of composition on the PDF curves of $(1-x)$PSW – (x)PT, x = 0, 0.15, 0.25, 0.35 and $(1-x)$PSW – (x)PZ, x = 0.15, 0.35 is displayed in Fig. 5. The most apparent change in $G(r)$ of PSW–PT is the alternation of amplitudes for B–O and Pb–B peaks at $r \approx 4.6$ Å and $r \approx 5.0$ Å. However, this is only a compositional effect due to the negative scattering length of Ti. The impact of Ti is noticeable also on the fi rst B–O peak, which becomes narrower with x and develops a split at its left side foot. Because of the negative value of b_{Ti}, the Ti–O distance in the (0.65)PSW–(0.35)PT is represented by a local minimum at $r \approx 1.9$ Å. This minimum is offset from the main B–O peak by ~0.2 Å, which is close to the difference of the radii of Sc and Ti ($\Delta R_\beta = 0.14$, $r_{\mathrm{Sc}^{3+}} = 0.745$ Å, $r_{\mathrm{Ti}^{4+}} = 0.605$ Å). Thus it is not possible to conclude without PDF modeling if there is any appreciable shift of the Ti atoms. Perhaps the most important structural feature in the compared curves is the alternation of the second peak at $r \approx 2.8$ Å, which is formed by Pb–O and O–O lengths. For PSW it has a right-side shoulder, then shows very broad, diffuse profi le at the Ti compositions of $x = 0.15, 0.25$ and fi nally re-develops a shoulder at $x = 0.35$. The observed "ruggedness" of the Pb–O peak coincides with the temperature of permittivity maximum $T_{\varepsilon,max}$. The broad, diffuse Pb–O peak at x =0.15, 0.25 suggests more randomness and shorter correlation length of the Pb displacements, which appears consistent with the drop in $T_{\varepsilon,max}$. A similar trend can be observed in the PSW–PZ

Downloaded 02 May 2005 to 165.123.34.86. Redistribution subject to AIP license or copyright, see http://proceedings.aip.org/proceedings/cpcr.jsp

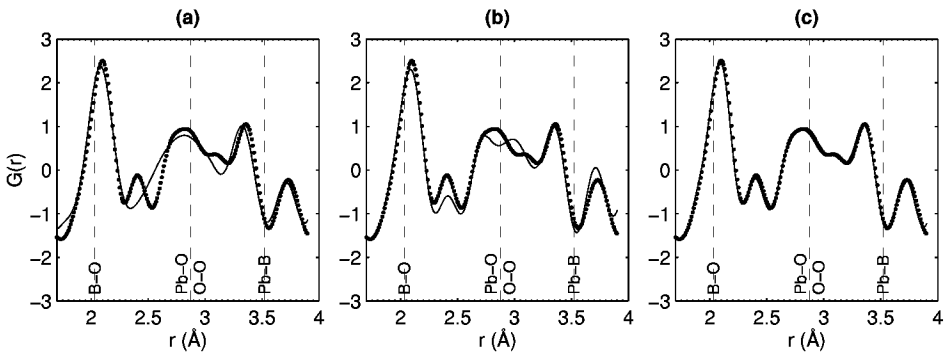

FIGURE 6. Simulated (solid line) and measured (dots) PDF for PSW. **(a)** [100] Pb shifts, **(b)** [100] Pb shifts and BO_6 rotations around $[10\bar{1}]$, **(c)** [100] Pb displacements with arbitrary shifts of oxygens.

system, where the "ruggedness" of the main Pb–O peak grows with the substitution of Zr, accompanied by the increase in $T_{\varepsilon,max}$.

4. MODELING AND DISCUSSION

The models of local structure used a $2 \times 2 \times 2$ periodic cell based on the average structure. All temperature coeffi cients were refi ned as isotropic, with a separate factor for the Sc-rich and mixed-cation β-sites. Several simple models of Pb and O displacements had been examined, and their magnitudes, PDF scale factor and temperature coeffi cients were fi tted to the experimental data.

In the fi rst model, the Pb cations were allowed to shift along [100], [110], [111] and $\pm$[111], in an anti-parallel pattern from β' to β'' sites. The oxygens could move in the B–O direction by changing the size of the BO_6 octahedra. The best fi t for 20 K data was always obtained by the model using [100] Pb displacements, which nicely reproduced the doubled peak of Pb–B distances, Fig. 6(a). Since the average position of Pb is in the center of the B_8 cube, its shift in the [100] direction creates 4 short and 4 long Pb–B lengths, as observed in the experiment. However, this model performs poorly for the Pb–O distances, where it could not replicate the shortest Pb–O distance of 2.4 Å. Therefore additional O displacements were introduced by allowing rotations of the BO_6 octahedra. General rotations of 8 connected octahedra in a $2 \times 2 \times 2$ cell, are described by 6 parameters, e. g. by two axes r, s at [0 0 0] and [0.5 0.5 0.5], and their rotation angles. However, the refi nement of all 6 parameters was numerically unstable, and the rotation axes had to be fi xed in some special directions. These were chosen as (i) $r = s = [10\bar{1}]$, (ii) $r = s = [\bar{2}11]$ and (iii) $r = [10\bar{1}]$, $s = [\bar{2}11]$. The type (i) rotation shifts 4 oxygens of the O_{12} cage directly to the Pb in the center, while the remaining 8 oxygens move away. The rotation (ii) creates the largest difference between the shortest and longest Pb–O lengths, and (iii) is a combination of the previous types. The best results were obtained using type (i) rotation, especially in the shorter range of PDF for 1.7Å $< r <$ 3.9 Å, as presented in Fig. 6(b). Although the BO_6 rotations were able to reproduce the

Downloaded 02 May 2005 to 165.123.34.86. Redistribution subject to AIP license or copyright, see http://proceedings.aip.org/proceedings/cpcr.jsp

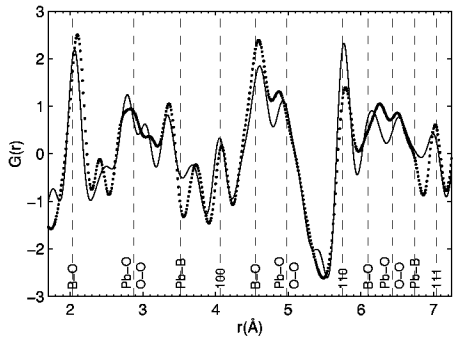

FIGURE 7. PDF for DFT simulation of PSW, dots mark the experimental data.

TABLE 2. Average cation displacements from DFT calculations

x	d_{Pb} (Å)	$d_{W,Ti}$ (Å)	$T_{\varepsilon,max}$ (°C)
0.0	0.4253	0.1764	-14
0.25	0.3947	0.1764	-40
0.625	0.3260	0.1895	244
1.0	0.4150	0.2851	490

shortest Pb–O distance, the overall agreement with the Pb–O peak was far from perfect. In addition, when the refi nement range was expanded to 8 Å, the rotation angles were considerably diminished and the agreement at short distances was lost. Displacements of the B cations were attempted, but they failed to induce any appreciable change in the PDF. It appeared that the real oxygen displacements were more random than allowed by the constraints of BO_6 rotations, with weak correlations even within the basic perovskite cell. Such structure was simulated by allowing all oxygens to shift arbitrarily, and the PDF of this model could be refi ned to a perfect agreement with the experimental data, see Fig. 6(c). The components of O shifts longitudinal to B–O were found to be about 2 times shorter than the transversal ones. The reliability of the simulated structures was verifi ed by calculating the bond valence sums [8]. For the fi nal structures the bond valence sums deviated from their ideal values by ~0.2 - ~0.6, which is similar or greater than for the initial Rietveld structure. This suggests that models for the local displacement can be improved and this work is currently in progress.

The experimental PDF data were also used to test the results of ab-initio density functional theory (DFT) simulations of the PSW–PT system. Calculations were performed using a $2 \times 2 \times 2$ or $3 \times 2 \times 2$ cell with periodic boundary conditions. The system energy was evaluated using a local density approximation exchange-correlation functional and minimized with respect to the atomic coordinates. The DFT calculations were carried out for 4 compositions with $x = 0$, 0.25, 0.625 and 1.0 and respective chemical formulas of $Pb_{12}[Sc_8W_4]O_{36}$, $Pb_8[Sc_4W_2Ti_2]O_{24}$, $Pb_8[Sc_2W_1Ti_5]O_{24}$ and $Pb_8Ti_8O_{24}$. Comparison of the DFT simulation of PSW with the experimental PDF is shown in Fig. 7. The calculated curve agrees well with the experimental data and essentially all of the peak positions are reproduced. The model structure of PSW had just one arrangement of the B cations, which was periodically repeated. Many more arrangements are possible in the real structure and their absence may account for the differences between the calculated and experimental curves. The average magnitudes of Pb and B-cation displacements with respect to their oxygen cage are listed in Table 2. The calculated cation shifts hint at a possible mechanism for the changes in $T_{\varepsilon,max}$. For $x < 0.25$ the displacements of the active W and Ti cations remain constant, possibly due to the absence of Ti–O–Ti or W–

Downloaded 02 May 2005 to 165.123.34.86. Redistribution subject to AIP license or copyright, see http://proceedings.aip.org/proceedings/cpcr.jsp

O–Ti clusters. At the same time the Pb shifts decrease together with the unit cell volume and the value of $T_{\varepsilon,max}$ drops. For a larger Ti content, the W and Ti displacements show signifi cant growth and their contribution to the dielectric response may become dominant, canceling the impact of decrease in Pb shifts. For a compositions close to PT long range ferroelectric domains with uniform Ti shifts are established, which may couple with the Pb cations and allow their shifts to grow back.

5. CONCLUSIONS

By carrying out synchrotron x-ray and neutron diffraction it was concluded that the average structure of PSW–PT and PSW–PZ, $x \leq 0.35$ systems is cubic with a "random site" arrangement of the B-cations. The Rietveld analysis confi rmed almost complete B-site order in the solid solution of PSW–PT for $x \leq 0.25$. On the local scale the crystal structure is considerably distorted from the average lattice. The distortion is realized through displacements of Pb and O atoms, while the B-cations remain at their average positions. The short-range PDF can be approximated by uniform Pb shifts in [100] direction and bound rotations of BO_6 octahedra around $10\bar{1}$ axis. For a longer range the O shifts need to be more random, however their major components are in the plane perpendicular to the B–O bond. The DFT simulated structure of PSW displayed a good agreement with the experimental PDF. The DFT results indicate that a possible reason for the decrease in $T_{\varepsilon,max}$ in the PSW–PT at $x < 0.25$ is a reduction of Pb displacements, before the contributions from the off-centering of Ti take over the dielectric response.

ACKNOWLEDGMENTS

The authors thank Dr. Beatriz Noheda from the NSLS, Brookhaven National Lab and Dr. Simine Short from the IPNS, Argonne National Lab for help with the experiments. The NSLS and IPNS are supported by the Department of Energy, Division of Materials Sciences and of Chemical Sciences. This work was funded by the Office of Naval Research through grant N00014-01-1-0860.

REFERENCES

1. Juhás, P., Davies, P. K., and Akbas, M. A., "Chemical Order and Dielectric Properties of Lead Scandium Tungstate Relaxors," in *AIP Conference Proceedings*, American Institute of Physics, 2002, vol. 626, pp. 108–116.
2. Larson, A. C., and von Dreele, R. B., *GSAS*, Los Alamos National Laboratory, Report LAUR 86-748 (2000).
3. Peterson, P. F., Gutmann, M., Proffen, T., and Billinge, S. J. L., *J. Appl. Crystallogr.*, **33**, 1192 (2000).
4. Proffen, T., and Billinge, S. J., *J. Appl. Crystallogr.*, **32**, 572–575 (1999).
5. Egami, T., *Mater. T. JIM*, **31**, 163–176 (1990).
6. Toby, B. H., and Egami, T., *Acta Crystallogr. A*, **A48**, 336–46 (1992).
7. Billinge, S. J. L., *Local Atomic Structure and Superconductivity of $Nd_{2-x}Ce_xCuO_4$: A Pair-Distribution-Function Study*, Ph.D. thesis, University of Pennsylvania (1992).
8. Brese, N. E., and Okeeffe, M., *Acta Crystallogr. B*, **47**, 192–197 (1991).

Downloaded 02 May 2005 to 165.123.34.86. Redistribution subject to AIP license or copyright, see http://proceedings.aip.org/proceedings/cpcr.jsp